Pulsed Electrical Field Ablation Plus Intratumoral Immunotherapy for Hepatocellular Carcinoma

Erik Soule, Carlos Vargas,† Ramon Sanchez,† Eduardo Cortes,† Nathan Goodyear,† Renata Barco,† and Jason Williams†*

Abstract: The fourth leading cause of cancer death worldwide, hepatocellular carcinoma, is known to progress relentlessly and recur despite treatment. Given the high tumor mutational burden, hepatocellular carcinoma is an attractive target for immunotherapy. Early trials of systemic checkpoint inhibitors have produced promising results, although complete and durable immunologic tumor eradication remains elusive. Pulsed electrical field ablation is a nonthermal ablation technology that causes apoptosis of diseased cells, while preserving the neoantigens for subsequent immune recognition by antigen-presenting cells and effectors. The neoantigens are released when the membrane is permeabilized. Furthermore, pulsed electrical field ablation was shown to induce the formation of tertiary lymphoid structures, congregations of immune cells that form inside the tumor at the ablation site, analogous to a lymph node. We present a novel treatment regimen with pulsed electrical field ablation combined with intratumoral immunotherapy injection. Treatments were performed using computed tomography guidance in a percutaneous manner. Pulsed electrical field ablation was performed within the tumor using the Aliya pulsed electrical field system (Galvanize, Redwood City, CA). After ablation was performed, the immunotherapy was administered into the tumor, mixed with iodinated contrast for visibility and gelfoam slurry for local retention. Three patients underwent treatment, and all treated tumors responded favorably with a decrease in size and a marked decrease in post-contrast enhancement. There were no treatment-related complications or high-grade toxicities. Pulsed electrical field ablation plus intratumoral immunotherapy may be safe and effective for the treatment of advanced hepatocellular carcinoma.

Key Words: hepatocellular carcinoma, pulsed electrical field ablation, immunotherapy, tumor microenvironment, tumor mutational burden, abscopal effect, tumor infiltrating lymphocytes

(*J Immunother* 2026;49:214–224)

KEY POINTS

What is already known on this topic—hepatocellular carcinoma may respond to immunotherapy, although the disease process continues to be a major cause of mortality worldwide.

What this study adds—pulsed electrical field ablation plus intratumoral immunotherapy may be safe and effective for hepatocellular carcinoma. Treated tumors and responsive satellite lesions became cystic and lost hypercellularity over time evidenced by progressive development of T2 hyperintensity and loss of restricted diffusion. The responsive tumor additionally became hypoattenuating with negligible radiotracer uptake on PET/CT imaging. A similar effect was seen on tumor thrombus. No complications or adverse events were observed.

How this study might affect research, practice, or policy—further investigation and refinement of a pulsed electrical field with intratumoral immunotherapy protocol in the context of a clinical trial may be warranted, given robust effectiveness and negligible toxicity.

The liver is a remarkable organ that may endure many years of chronic hepatitis before its regenerative capacity is finally exhausted and cirrhosis occurs. Hepatocellular carcinoma (HCC) is the dreaded end-stage complication of hepatic cirrhosis. HCC carcinogenesis is multifactorial but increases exponentially in the cirrhotic liver. This is postulated to be due in part to the loss of replicative capacity in the cirrhotic liver due to telomere shortening and accumulation of senescent hepatocytes. Given that liver mass is tightly regulated via incompletely understood mechanisms, impaired replicative capacity of normal hepatocytes allows a niche for proliferation of premalignant cells. These cells may harbor a mutation in p53 or another tumor-suppressor gene, which allows them to resist apoptosis, accumulate mutations, and ultimately progress to HCC.[1] A telomerase mutation may eventually result in immortalization of the HCC clone, with deleterious consequences for the host organism.[2] Owing to the accumulation of chromosomal abnormalities during carcinogenesis, HCC has a tumor mutational burden (TMB) that ranks 12th among 30 different cancer types studied, relatively high.[3] TMB is a predictive biomarker for response to immunotherapy: indeed, trials of systemic immunotherapy and combination therapy have yielded promising results.[4] Available treatment options ultimately fall short of the ideal result, reliable, complete, and durable eradication of HCC with negligible toxicity.

HCC is the sixth most common malignancy and the fourth leading cause of cancer death worldwide. HCC will continue to constitute a major public health problem, especially in developed countries, where the prevalence of obesity and hepatic steatosis continues to increase.[5] Current standard of care clinical treatment for HCC includes resection, transplantation, and ablative therapies for early-stage tumors. Late-stage tumors may receive intra-arterial and systemic treatments. Ultimately, the overarching treatment goal is to allow the patient to survive until liver transplantation. Multidisciplinary collaboration is used to achieve this goal with multiple modalities,

Received for publication September 3, 2025; accepted November 20, 2025.

From the *University of Florida College of Medicine–Jacksonville, Jacksonville, FL; and †Williams Cancer Institute, Beverly Hills, CA.

Reprints: Jason Williams, Williams Cancer Institute, 9777 Wilshire Blvd, Ste 1004, Beverly Hills, CA 90212 (e-mail: cancerablation7@gmail.com).

Copyright © 2026 Wolters Kluwer Health, Inc. All rights reserved.

DOI: 10.1097/CJI.0000000000000596

Copyright © 2026 Wolters Kluwer Health, Inc. All rights reserved.

TABLE 1. Laboratory Studies - Patient 1

	Patient 1—pretreatment (5 mo)	Patient 1—pretreatment (1 mo)	Patient 1—posttreatment (5 mo)
Complete blood count			
Red blood cells (10^6/μL)	5	4.77	3.88
White blood cells (10^3/μL)	6.25	3.84	2.2
Hemoglobin (g/dL)	15.2	14.5	11.4
Hematocrit (%)	45	44	33.9
Platelets (10^3/μL)	202	66	43
Comprehensive metabolic panel			
Glucose (mg/dL)	Not available	138	199
Calcium (mg/dL)	Not available	Not available	9.7
Sodium (mmol/L)	Not available	Not available	135
Potassium (mmol/L)	Not available	Not available	4.2
Chloride (mmol/L)	Not available	Not available	103
Bicarbonate (mmol/L)	Not available	Not available	25
Blood urea nitrogen (mg/dL)	Not available	Not available	11
Creatinine (mg/dL)	Not available	0.68	0.71
ALT (U/L)	Not available	44	22
AST (U/L)	Not available	63	32
Alkaline phosphatase (U/L)	Not available	154	199
Bilirubin (mg/dL)	Not available	0.62	0.7
Albumin (g/dL)	Not available	4.39	4.4
Alpha fetoprotein (ng/mL)	44,0217	17.4	4.1
International normalized ratio	Not available	Not available	Not available
Prothrombin level (mAU/mL)	18,052	33	Not available

ultimately contributing to keeping disease burden in check while preserving hepatic reserve.[6] Significant strides have been made in finding new, innovative ways to accomplish these objectives via locoregional therapy. We present a novel locoregional therapy incorporating percutaneous pulsed electrical field ablation with intratumoral immunotherapy injection that has achieved promising results in a small cohort of 3 patients.

MATERIALS AND METHODS

Hepatocellular carcinoma was diagnosed with tissue sampling, or using the established LI-RADS criteria, namely that an arterially enhancing hepatic lesion with washout on delayed phase in the cirrhotic liver can be diagnosed as LI-RADS category 5, or "definitely HCC." Treatments were performed using CT-guidance in a percutaneous manner. Pulsed electrical field (PEF) ablation was performed within the tumor for 1–8 cycles using the Aliya PEF system (Galvanize, Redwood City, CA). After ablation was performed, the immunotherapy mixture was administered into the tumor under CT guidance, mixed with iodinated contrast for visibility and gelfoam slurry for local retention. All patients received 1–3 treatments, with ~2–4 weeks between treatments.

The injected agents were used off-label and selected for their mechanisms of action. The goal was to elicit immunologic tumor elimination via multiple pathways. The following agents were injected. Ionic liquid—vehicle for delivery of immunotherapy with enhanced tissue permeation and local retention.[7] Freund's adjuvant—heat-killed mycobacterium mixed in oil and water. Used as a vehicle for delivery of immunotherapy with increased local retention and multiple immunostimulatory properties, including dendritic cell activation.[8] CpG—an oligodeoxynucleotide which activates TLR9 signaling, resulting in activation of multiple lineages of immune cells, including

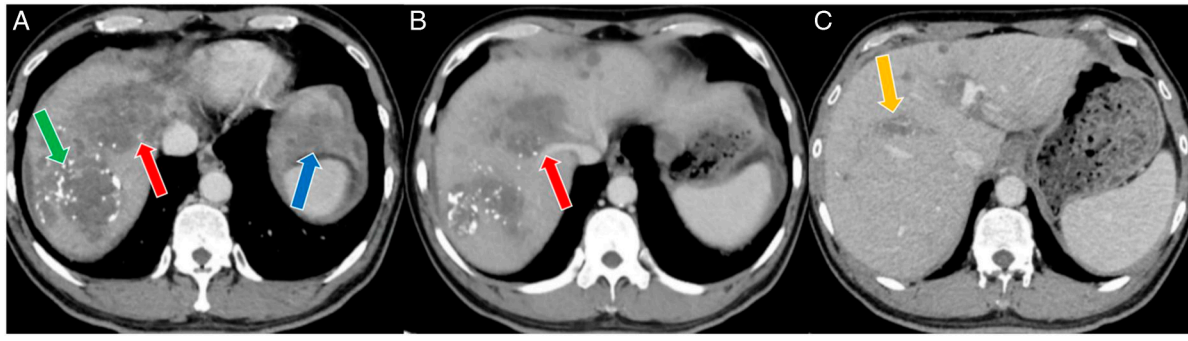

FIGURE 1. Pretreatment (1 mo) imaging (A–C) with contrast-enhanced CT demonstrated lipiodol staining of the lesion in hepatic segment VII previously treated with TACE (green arrow). There is a large infiltrative lesion in segment IVa/VIII (red arrows). An additional suspicious lesion was identified in segment II (blue arrow). Finally, a filling defect in the right anterior portal vein was suspicious for thrombus (orange arrow). The portal thrombus was documented to represent an enhancing tumor thrombus on the radiology report of a prior (4 mo) contrast-enhanced CT scan of the abdomen, but those images are not available.

Copyright © 2026 Wolters Kluwer Health, Inc. All rights reserved.

Copyright © 2026 Wolters Kluwer Health, Inc. All rights reserved.

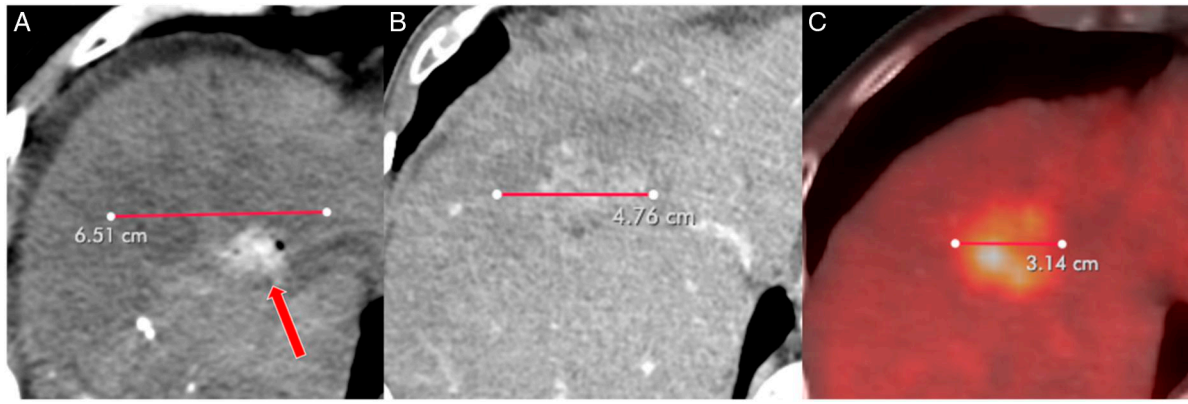

FIGURE 2. Intratumoral treatment and subsequent treatment response. Immediate postprocedural noncontrast CT (A) demonstrates an infiltrative appearing tumor with very limited tissue contrast measuring ~6.5 cm in transverse dimension. Expected posttreatment changes are appreciated (red arrow). Postcontrast CT (B) at 5 months follow-up demonstrates an enhancing tumor measuring ~4.8 cm in transverse dimension. PET/CT performed at 8 months follow-up (C) demonstrates decreased size of the tumor measuring 3.1 cm in transverse dimension with low-level radiotracer uptake.

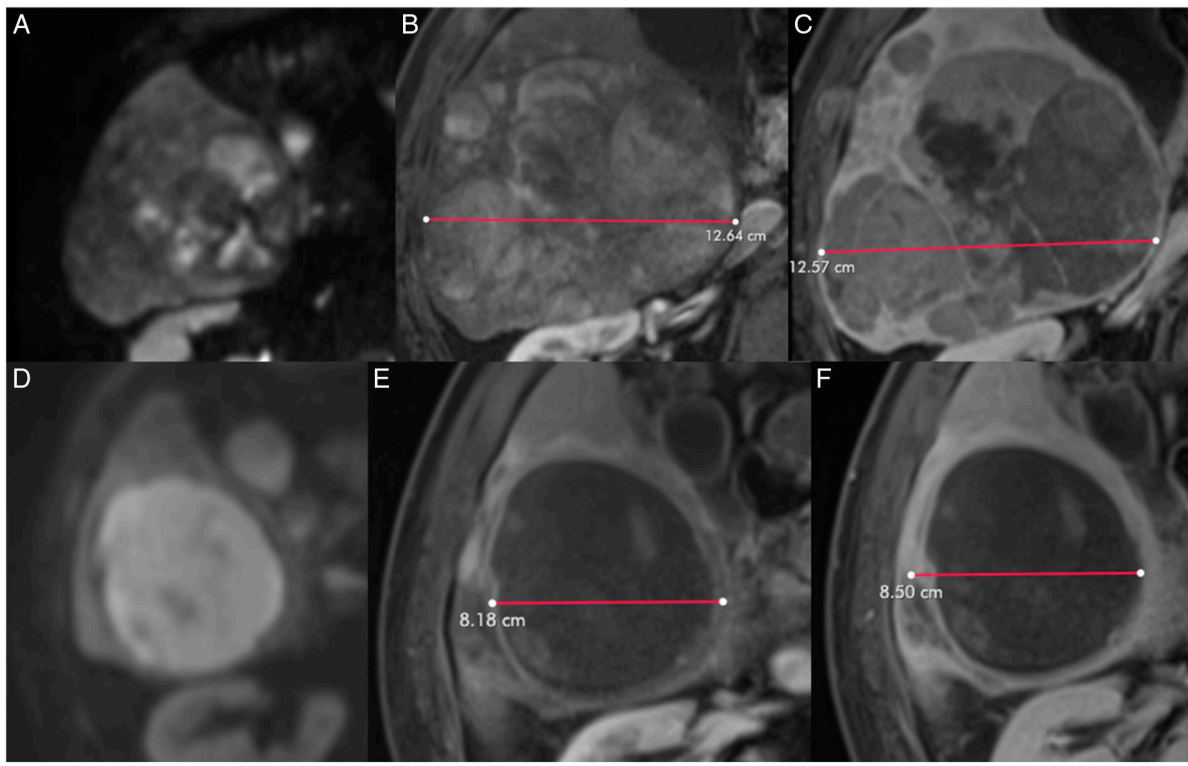

FIGURE 3. Early response to PEF ablation with intratumoral immunotherapy administration. Diffusion-weighted magnetic resonance imaging performed 5 months pretreatment (A) demonstrates heterogeneous hyperintensity of the large tumor in segment V/VI consistent with hypercellularity. Postcontrast T1-weighted fat-suppressed MRI performed 1 month pretreatment in early and delayed phase (B, C) demonstrates heterogeneously enhancing tumor with innumerable satellite lesions and washout on delayed phase, measuring ~12.6 cm in transverse dimension in aggregate. Note the rapid doubling time consistent with aggressive biologic behavior. Diffusion-weighted magnetic resonance imaging performed at 6 months posttreatment follow-up (D) demonstrates a relatively homogenous T2 shine-through artifact without a hypointense signal on the corresponding ADC map (not shown). Postcontrast T1-weighted fat-suppressed MRI in early and delayed phase at 6 months follow-up (E, F) demonstrates reduced tumor bulk and markedly decreased enhancement. Morphology of the tumor is also altered with encapsulation and consolidation of satellite lesions into a single cystic mass. At this time point, the tumor measures ~8.5 cm in transverse dimension.

Copyright © 2026 Wolters Kluwer Health, Inc. All rights reserved.
Copyright © 2026 Wolters Kluwer Health, Inc. All rights reserved.

TABLE 2. Laboratory Studies - Patient 2

	Patient 2—pretreatment (day of 1st treatment)	Patient 2—day of 3rd treatment	Patient 2—posttreatment (6 mo)
Complete blood count			
Red blood cells (10^6/μL)	4.97	5.09	5.32
White blood cells (10^3/μL)	5.02	4.33	5.82
Hemoglobin (g/dL)	12.9	13.3	13.5
Hematocrit (%)	40.4	40.6	40.9
Platelets (10^3/μL)	199	131	111
Comprehensive metabolic panel			
Glucose (mg/dL)	106.2	117	131.8
Calcium (mg/dL)	9	9.1	9.3
Sodium (mmol/L)	138.7	138.2	142.5
Potassium (mmol/L)	4.3	3.8	4
Chloride (mmol/L)	102.5	104	106.8
Bicarbonate (mmol/L)	Not available	Not available	Not available
Blood urea nitrogen (mg/dL)	10.8	7.67	20.06
Creatinine (mg/dL)	0.66	0.56	0.63
ALT (U/L)	40	124.7	37.2
AST (U/L)	67.2	181.1	39.8
Alkaline phosphatase (U/L)	138.5	161.7	Not available
Bilirubin (mg/dL)	0.64	0.74	0.72
Albumin (g/dL)	3.46	3.49	4.13
Alpha fetoprotein (ng/mL)	Not available	Not available	Not available
International normalized ratio	1.25	Not available	1.22

NK cells, T cells, and B cells.[9] Gemcitabine—integrates into DNA, causing apoptosis, boosts immune response via effects on antigen-presenting cells as well as effector cells.[10] Evofosfamide—hypoxia-activated prodrug to target hypoxic regions of the tumor, where it is converted into a cytotoxic metabolite. May be synergistic with checkpoint-inhibitor immunotherapies.[11] Onivyde—liposomal formulation of irinotecan, a topoisomerase I inhibitor that causes DNA damage and apoptosis.[12] Gallotannin—a hydrolysable tannin, which may inhibit JAK/STAT signaling in cancer cells and induce apoptosis or senescence.[13] Selenium—an essential trace element that may reverse immunosuppression in the tumor microenvironment and activate effectors.[14] PV-10 (Rose Bengal)—a water-soluble xanthene dye with immunostimulatory properties when injected intratumorally, and synergy with other classes of immunotherapy.[15] Parecoxib—COX-2 inhibitor, reduces prostaglandin activity and demonstrates synergy with immunotherapy.[16] Anti-CD47 (antagonist)—a monoclonal antibody that binds and inactivates CD47. CD47 may be overexpressed on the cell membrane of tumor cells and enable those cells to evade immune surveillance via the blockade of phagocytic mechanisms.[17] CD40L, anti-CD40 (agonist)—a monoclonal antibody that mimics CD40L, resulting in costimulatory signaling at immune synapses. This activates dendritic cells, leading to proliferation of effectors.[18] Anti-OX40 (agonist)—a monoclonal antibody that binds and activates OX40, a costimulatory molecule. This may increase survival and proliferation of effectors and may suppress regulatory T cells.[19] Anti-CD276 (antagonist), anti-B7-H3 (antagonist)—monoclonal antibodies that bind and inactivate the B7-H3 (also known as CD276) protein, which is overexpressed in the tumor microenvironment. This immune checkpoint molecule may attenuate the activity of effectors and promote an immunosuppressive tumor microenvironment.[20] Yervoy—a monoclonal antibody that binds to the CTLA-4 immune checkpoint molecule, inactivating it. This leads to increased effector activity via multiple mechanisms.[21] Anti-4-1BB (agonist)—a monoclonal antibody that binds the 4-1BB costimulatory surface receptor expressed on activated T cells. This may result in increased effector survival, proliferation, and effector function.[22] Anti-CSF1R (antagonist)—a monoclonal antibody that binds to and inactivates the CSF1R protein. CSF1R is a tyrosine kinase transmembrane receptor that induces the development of immunosuppressive tumor-associated macrophages.[23] SX-682—a small molecule inhibitor of CXCR1/2, chemokine receptors responsible for recruitment of immunosuppressive myeloid-derived suppressor cells into the tumor microenvironment.[24] AOH-1190—a small molecule inhibitor of PCNA (proliferating cell nuclear antigen), a protein that promotes cancer cell growth and proliferation.[25] Anti-LAG3 (antagonist)—an inhibitory monoclonal antibody specific for LAG3. LAG3 is expressed on tumor-infiltrating lymphocytes and its activation reduces effector activity and proliferation.[26] Opdivo—a monoclonal antibody that binds to the immune checkpoint PD-1 receptor, inhibiting it and facilitating effector activity.[27] Anakinra—a recombinant interleukin-1 receptor antagonist. Counteracts the IL-1 signaling pathway, which has been implicated in tumor progression.[28,29] Tocilizumab—a monoclonal antibody that binds to and inhibits the IL-6 cytokine. IL-6 signaling may promote immunosuppression in the tumor microenvironment.[30] Dosages of the checkpoint inhibitors administered intratumorally were significantly lower than those indicated for systemic immunotherapy.

RESULTS

Patient 1

A patient in their 50s who underwent 2 treatments, without PEF due to commercial unavailability at the time of treatment. This patient was diagnosed with HCC based

Copyright © 2026 Wolters Kluwer Health, Inc. All rights reserved.

Copyright © 2026 Wolters Kluwer Health, Inc. All rights reserved.

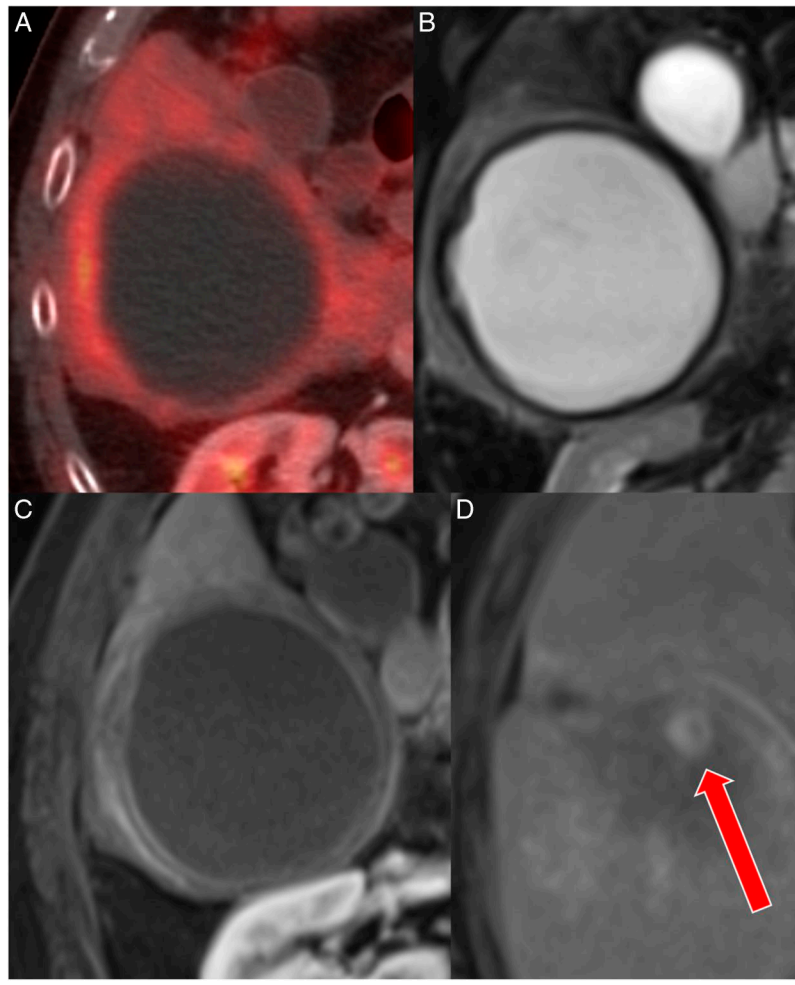

FIGURE 4. Continued long-term imaging follow-up. Fluorodeoxyglucose PET/CT (A) obtained at 14 months follow-up demonstrates no evidence of radionuclide uptake within the treated lesion, which is now fluid attenuation. T2 fat-suppressed MRI (B) at 18 months follow-up demonstrates that the mass is now uniformly T2 hyperintense, consistent with cystic change. Arterial phase MRI (C) demonstrates no enhancement of the lesion, except for a small nodule at the apex (D), which has remained stable in size and morphology on serial imaging.

on the presence of chronic hepatitis B infection and the imaging findings consistent with LI-RADS-TIV category. The presence of an extensive infiltrative tumor in both lobes and portal venous invasion placed him in the BCLC category D. Initially, at diagnosis, he was likely Child-Pugh B with significant liver dysfunction. He did receive TACE followed by 4 months of PD-1 checkpoint inhibitor monotherapy. At the time of his first treatment, his laboratory derangements had improved significantly (Table 1), but there was an incomplete radiologic response (Fig. 1). The first treatment was performed with intratumoral administration of ionic liquid, Gemcitabine, Evofosfamide, Gallotannin, Selenium, PV-10, CD-47, CD-40, OX-40, CD-276, Yervoy, CpG, and Freund's adjuvant. The second treatment was performed 10 days after the first with administration of ionic liquid, Gemcitabine, Selenium, PV-10, CD-47, CD-40, OX-40, CD-276, Yervoy, CpG, and Freund's adjuvant.

The patient developed moderate-volume ascites after the second treatment, which quickly resolved. Postprocedural laboratory studies were significant for continued normalization of AFP to 4.1 ng/mL at 5 months. The tumor demonstrated decreased size on an 8-month follow-up PET/CT and was mildly tracer-avid (Fig. 2). An additional PET/CT performed at 20 months follow-up demonstrated continued treatment response with continued decrease in size and radiotracer uptake, although those images are not available for review. The patient continues to undergo regular follow-up 3.5 years posttreatment, with normal AFP and a complete radiologic response.

Patient 2

A patient in their 50s presented with a very large tumor and numerous satellite lesions. The patient had a history of iron overload and liver cirrhosis, diagnosed based on imaging findings. There was a family history of hemochromatosis in the patient's father. The tumors were enhancing arterially with washout on delayed imaging, consistent with LI-RADS 5 classification. He received systemic therapy with bevacizumab and atezolizumab for 9

Copyright © 2026 Wolters Kluwer Health, Inc. All rights reserved.
Copyright © 2026 Wolters Kluwer Health, Inc. All rights reserved.

TABLE 3. Laboratory Studies - Patient 3

	Patient 3—pretreatment (day of treatment)	Patient 3—posttreatment (day of treatment)	Patient 3—posttreatment (10 d)
Complete blood count			
Red blood cells (10^6/μL)	3.95	2.72	3.16
White blood cells (10^3/μL)	8.89	4.1	16.78
Hemoglobin (g/dL)	11.3	7.9	9.3
Hematocrit (%)	34.5	25.6	27.7
Platelets (10^3/μL)	165	140	155
Comprehensive metabolic panel			
Glucose (mg/dL)	Not available	69.5	138.7
Calcium (mg/dL)	Not available	8.5	8.6
Sodium (mmol/L)	Not available	138.4	140.1
Potassium (mmol/L)	Not available	3.5	5.3
Chloride (mmol/L)	Not available	106.68	109.69
Bicarbonate (mmol/L)	Not available	18.7	Not available
Blood urea nitrogen (mg/dL)	Not available	13.02	58.45
Creatinine (mg/dL)	Not available	0.84	1.88
ALT (U/L)	Not available	122	280
AST (U/L)	Not available	271.7	73.9
Alkaline phosphatase (U/L)	Not available	220.05	216.85
Bilirubin (mg/dL)	Not available	1.36	1.38
Albumin (g/dL)	Not available	3.08	3.35
Alpha fetoprotein (ng/mL)	Not available	Not available	Not available
International normalized ratio	0.98	2.35	Not available

weeks before treatment without a significant radiologic response. The patient was BCLC category B, Child-Pugh A, with a MELD 3.0 of 8 (Table 2). He underwent 3 treatments, the first was performed with 8 cycles of PEF followed by injection of CpG, 4-1BB, CD-40, CD-47, Csf-1r, Yervoy, SX-682, and Parecoxib. The second treatment was performed 27 days after the first with 7 cycles of PEF followed by 4-1BB, CD40L, CD-47, 4-1BB, CD-40, OX-40, CpG, Csf-1r, Yervoy, SX-682, AOH-1190, and Parecoxib. The third treatment was 38 days after the first, with 2 cycles of PEF followed by intratumoral administration of CD-47, CD-40, B7H3, CPG/Poly IC, Csf-1r, LAG-3, Yervoy, Opdivo, AOH-1190, and Parecoxib.

After treatment, the dominant tumor coalesced with the satellite lesions and arterial enhancement gradually resolved (Fig. 3). The tumor became T2 hyperintense on MRI and decreased in size over time. An attempt was made to drain the tumor due to concern for abscess formation. This yielded a small quantity of reddish-brown nonpurulent material containing thick debris. The material was sent for cytology, and the determination was made that there were no malignant cells present.

Additional follow-up was obtained with PET/CT, ultrasonography, and contrast-enhanced MRI. The cystic mass demonstrated continued decrease in size and enhancement at 18 months, except for a small enhancing nodule at its apex. The enhancing nodule has remained stable in size and morphology on serial imaging, consistent with a questionable recurrence. There was no radiotracer uptake on PET/CT, and no significant restricted diffusion (Fig. 4).

Patient 3

A patient in their 60s who presented with advanced disease, including extensive portal vein tumor thrombus. HCC was diagnosed with a CT-guided biopsy. An attempt was made to surgically resect the right lobe, which was ultimately aborted when invasion of the main portal vein was appreciated after surgical exposure. Portal vein tumor thrombus extended to the main portal vein at the level of the mesenteric veins, as well as to the left and right portal veins at the time of treatment. The patient was BCLC category C. He underwent 1 treatment with 3 cycles of PEF followed by intratumoral administration of CD-40, B7H3, CD-47, Csf-1r, 4-1BB, CpG, Yervoy, PD-1, Parecoxib, Anakinra, Onivyde, and Tocilizumab into a dominant mass in segment VII. Immediate postprocedure laboratory studies were significant for the development of lactic acidosis (7.09 mmol/L), which resolved gradually after 1 week. At the 1-week time point, there was a mild acute kidney injury (Table 3).

After the initial treatment, the patient was unfortunately lost to follow-up until ultimately presenting with biliary obstruction after 6 months. Outside imaging, obtained and reviewed retrospectively, demonstrated that the patient received a CT scan with portal and delayed phase at 6.5 weeks posttreatment. This demonstrated treatment-related changes to the dominant mass-forming portion of the tumor, which was without significant enhancement. PET/CT performed 6.5 months posttreatment showed no radiotracer uptake of the treated lesion and an adjacent responsive satellite lesion. There was a significantly decreased size of the treated mass and responsive satellite nodule at that time point (Fig. 5). The extensive tumor thrombus also demonstrated similar changes, with decreased size and lack of enhancement (Fig. 6).

Additional imaging was performed after the patient presented with biliary obstruction, demonstrating progression of infiltrative tumor in the inferior portion of the right lobe as well as invasion of infiltrative tumor at the porta hepatis. There was increased tumor thrombus, now to the level of the splenic hilum, invasive within the liver diffusely (Fig. 7). The overall response pattern likely represents an enestic response, where the injected tumor responded favorably; however, separate sites of disease ultimately progressed.

Copyright © 2026 Wolters Kluwer Health, Inc. All rights reserved.

Copyright © 2026 Wolters Kluwer Health, Inc. All rights reserved.

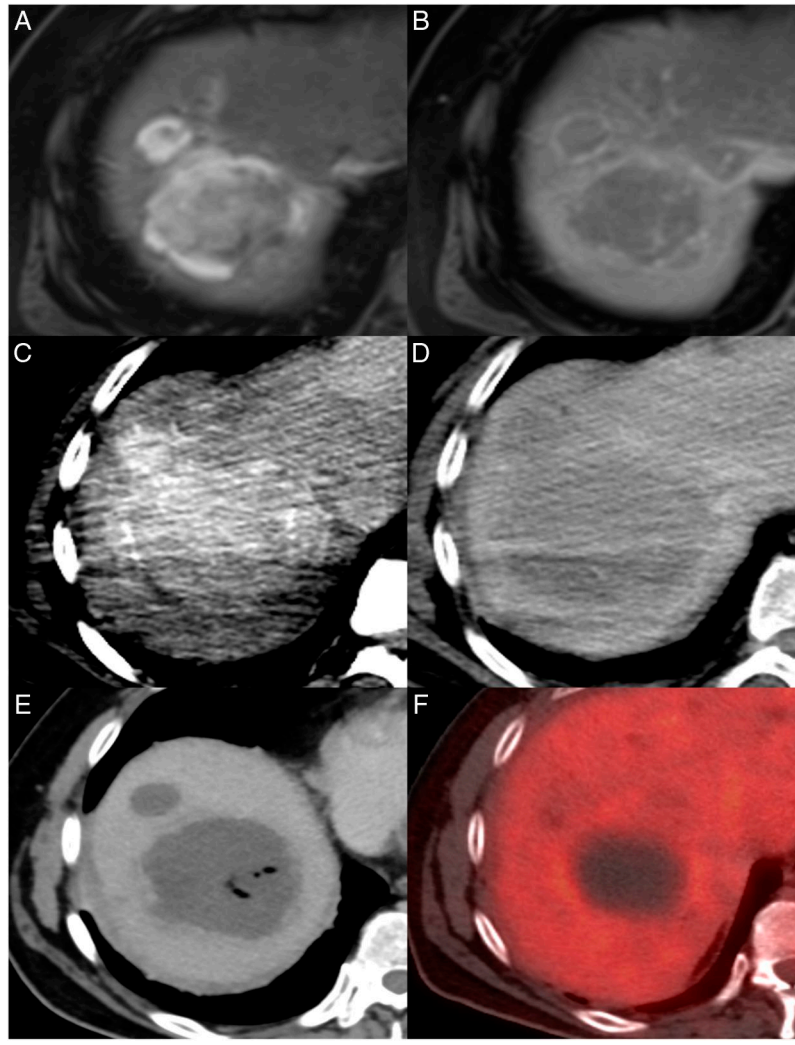

FIGURE 5. Imaging response of treated tumor. Fat-suppressed postcontrast T1-weighted MRI performed 7 months before treatment in arterial (A) and delayed (B) phases demonstrates a bulky mass in segment VII/VIII with heterogeneous arterial enhancement, washout, and delayed-enhancing capsule. Intraprocedural contrast-enhanced computed tomography obtained at the time of treatment in arterial (C) and delayed (D) phases demonstrate progression of the lesions. Contrast-enhanced computed tomography obtained 6 weeks posttreatment (E) demonstrates treatment-related changes to the dominant segment VII hepatocellular carcinoma and adjacent untreated satellite lesion, characterized by intratumoral air/gelfoam, lack of enhancement, and modest shrinkage of both lesions. Further follow-up with 18-F fluorodeoxyglucose positron emission tomography at 6.5 months (F) demonstrates continued cystic necrosis and no significant radiotracer uptake.

DISCUSSION

We present a small cohort of 3 patients with HCC who were either deemed not surgical candidates or refused surgical treatment. One patient underwent surgery, but the tumor was not resected at that time. These patients underwent treatment with PEF ablation followed directly by intratumoral immunotherapy injection. Follow-up imaging demonstrated decreased size and enhancement of the treated tumors and satellite lesions. We hypothesize that this is due to recognition of tumor antigens by tumor-infiltrating lymphocytes (TIL) and subsequent systemic immunologic tumor elimination, or abscopal effect. HCC is known to have a relatively high TMB, making it a promising candidate for immunotherapy.[31] Early trials of systemic immunotherapy for HCC have yielded promising results, albeit limited by significant toxicity. Due to the field cancerization effect of hepatic cirrhosis and the inherent immunosuppressive nature of the hepatic tissue, a durable complete response remains elusive.[32] Our treatment protocol circumvents the limitation of systemic intravenous administration of immunotherapy by administering the pharmaceuticals directly into the tumor, which we postulate to immunomodulate the local microenvironment. Furthermore, pretreating the area with PEF ablation causes the malignant cells to release their mutated-self antigens (neoantigens) when their cell membranes are rendered incompetent for subsequent immune recognition. PEF ablation is poised to shift the treatment paradigm for advanced malignancy across tumor types, given its relative safety and emerging evidence that it may significantly

Copyright © 2026 Wolters Kluwer Health, Inc. All rights reserved.
Copyright © 2026 Wolters Kluwer Health, Inc. All rights reserved.

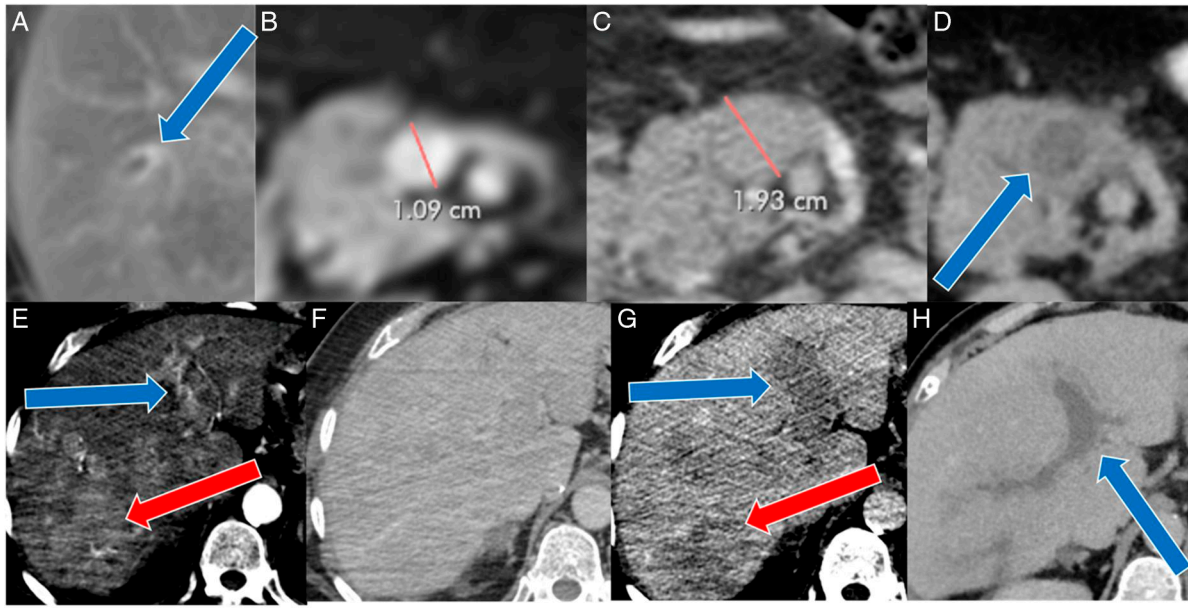

FIGURE 6. Imaging response of tumor thrombus. Postcontrast fat-suppressed T1-weighted MRI (A) performed 7 months before treatment demonstrates a filling defect in a branch of the right portal vein (blue arrow) associated with the dominant mass in segment VII. The portal circulation at the level of the first jejunal branch (B) measures 1.09 cm at that time and demonstrates enhancement consistent with patency. Intraprocedural computed tomography performed in the portal venous phase (C) at the level of the first jejunal branch demonstrates enlargement of the portal circulation to 1.93 cm, suspicious for thrombus. Computed tomography performed 6.5 weeks posttreatment in the portal venous phase (D) at the level of the first jejunal branch demonstrates treatment-related changes to the thrombus with decreased size and development of hypoattenuation (blue arrow). Intraprocedural computed tomography performed in arterial (E), portal venous (F), and delayed (G) phases demonstrate extensive tumor thrombus involving the left portal vein with arterial enhancement and delayed washout (blue arrows). Tumor thrombus was present throughout the portal vasculature bilaterally at the time of treatment, consistent with LI-RADS TIV (tumor in vein). Note the arterially enhancing infiltrative lesion in segment VI/VII with delayed washout (red arrows), and its lack of tissue contrast on the portal venous phase. Computed tomography at 6.5 weeks follow-up obtained in portal venous phase (H) demonstrates treatment-related changes to the left portal vein tumor thrombus, which may represent thrombus regression (blue arrow).

extend overall survival.[33] PEF was also shown to induce the development of tertiary lymphoid structures (TLS) in the ablation zone.[34] Our hypothesis is that these TLS served as scaffolds to attract TILs specific to HCC neoantigens. These TILs may be activated and induced to proliferate by the injected medications including CpG which stimulates the innate immune system and may act as a "danger signal," augmenting the immune response by inducing a proinflammatory microenvironment.[35] Additional medications included multiple checkpoint blockade, activation of antigen-presenting cells, and other pharmaceuticals, which have been shown to enhance anti-tumor immunity. Subsequent treatments may be synergistic in this mechanism, restimulating the response to the previously recognized neoantigens, and broadening the range of neoantigens targeted by the immune system due to intratumoral and intertumoral heterogeneity.

Promising effectiveness was demonstrated against mass-forming hepatocellular carcinomas in this cohort. This is evidenced by the progressive decrease in enhancement and size of the responsive tumors over time. These tumors also developed T2 hyperintensity, which progressed over time, as well as hypoattenuation on CT imaging consistent with cystic necrosis. Finally, the two responsive tumors that received PEF ablation demonstrated loss of previously seen restricted diffusion consistent with loss of hypercellularity and complete absence of radiotracer uptake on PET/CT consistent with negligible metabolic activity. Given the large size of the treated lesions, these patients would not be candidates for conventional curative treatments. Our treatment protocol, nonetheless, resulted in long-term survival and, ostensibly, no definite active disease in 2 of these patients. The third patient, unfortunately, had an advanced portal tumor thrombus present at the time of initial treatment and ultimately progressed. Tumor thrombus is a known risk factor for failure to achieve a complete response with immunotherapy combination treatments.[36] The treated mass, however, responded well to treatment and underwent cystic regression consistent with the treatment response of the other 2 patients. We postulate that treatment failure in this case was ultimately on the basis of intertumoral heterogeneity between the focal mass-forming treated tumor and a synchronous untreated infiltrative tumor. The tumor thrombus and infiltrative carcinoma did demonstrate a promising response, with decreased size of the infiltrative carcinoma and early regression of the tumor thrombus. This is certainly a promising finding, although we hypothesize that the infiltrative carcinoma had a different subset of neoantigens and immune-evasion mechanisms, which allowed it to "weather the storm" of immunologic tumor elimination. After the acute anti-tumor systemic immune response subsided, those surviving clones were able to resume invasion of the liver and portal vasculature. Infiltrative variant HCC is a grave problem

Copyright © 2026 Wolters Kluwer Health, Inc. All rights reserved.

Copyright © 2026 Wolters Kluwer Health, Inc. All rights reserved.

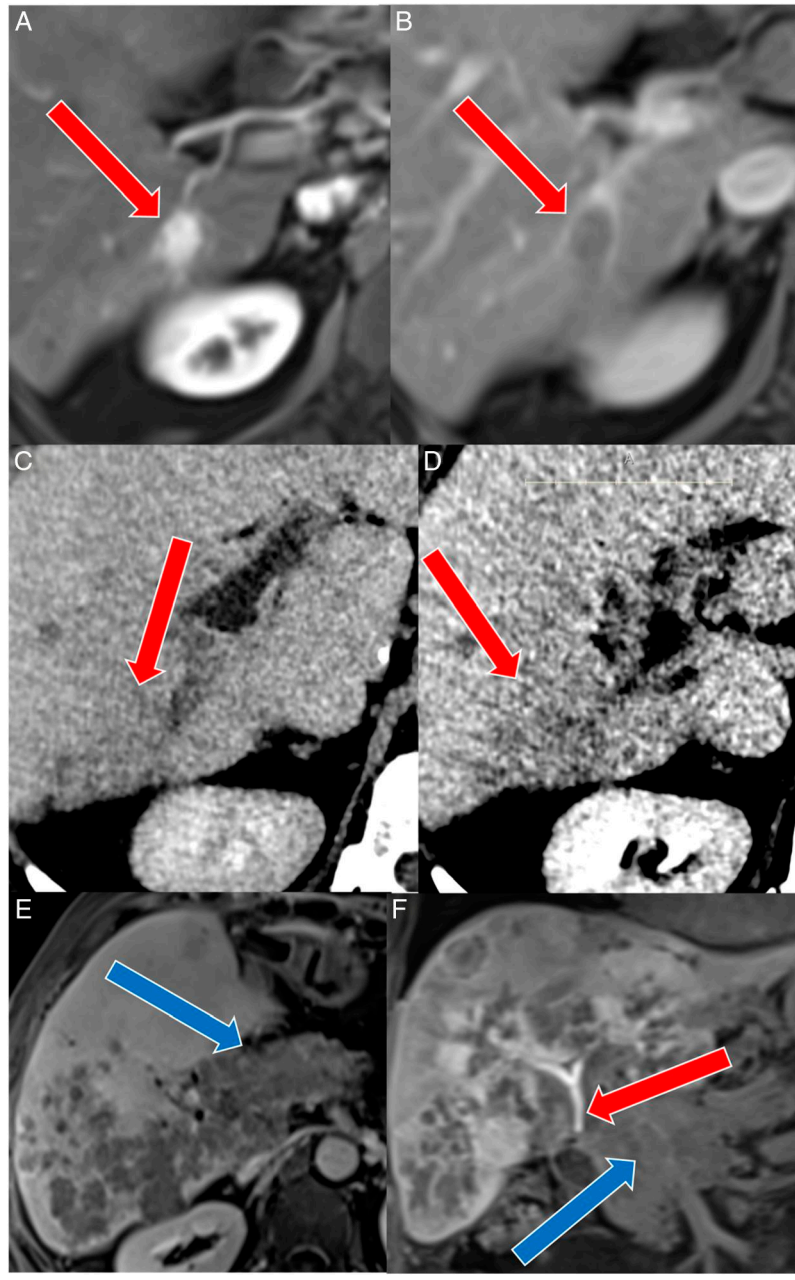

FIGURE 7. Synchronous untreated right lobe infiltrative hepatocellular carcinoma. Postcontrast axial T1-weighted fat-suppressed magnetic resonance imaging was performed 7 months before treatment in the arterial (A) and delayed (B) phase. Note the arterially enhancing HCC with delayed washout in segment VI (red arrows). Computed tomography 6.5 weeks posttreatment in the portal venous (C) and delayed (D) phases demonstrates that the mass did not show an analogous response to treatment (red arrows). This mass demonstrated very little tissue contrast in comparison to normal hepatic parenchyma on CT imaging. The infiltrative tumor, however, demonstrated a modest decrease in size compared with the intraprocedural time point. Delayed phase T1-weighted fat-suppressed axial postcontrast Eovist magnetic resonance imaging performed 5 months posttreatment (E, F) demonstrates extensive progression of the infiltrative segment VI lesion. There is portal venous tumor thrombus involving the entire splenic vein with diffuse invasive disease, including the porta hepatis (blue arrows), resulting in biliary obstruction (red arrow).

due to its aggressive nature and difficulties in recognition on imaging related to poor intrinsic tissue contrast. Patients would benefit from early follow-up with contrast-enhanced MRI at 3 months, obtained in arterial, portal venous, and delayed phases, and reviewed by an experienced, subspecialty-trained radiologist. Even under these ideal circumstances, infiltrative variant HCC may prove difficult to recognize prospectively.

Carcinogenesis, metastasis, and immune evasion are a clonal process, meaning that a tiny minority of tumoral

Copyright © 2026 Wolters Kluwer Health, Inc. All rights reserved.
Copyright © 2026 Wolters Kluwer Health, Inc. All rights reserved.

cells possess the potential to form distant metastases, known as cancer stem cells (CSC). This is a common mechanism of treatment failure, both with chemotherapy and immunotherapy. Under noxious posttreatment conditions, the bulk of the tumoral cells may die off, while CSCs may become quiescent and bide their time until conditions improve for growth, replication, local invasion, and ultimately distant metastasis.[37] This has implications in treatment with immunotherapy, especially for patients with multiple tumors or sites of metastatic disease. Some of the lesions may respond, while others may not, due to the clonal nature of the disease. The CSC progenitor of a given lesion may have resistance to the specific set of activated TILs due to an acquired mutation, antigen loss, or various other mechanisms.[38] This concept highlights the potential of this novel treatment protocol given that the treatment can be repeated if targetable tumor is present, theoretically widening the spectrum of neoantigens which are reacted against by TILs. Additional cancer-specific T-cell receptors may be recruited if PEF is performed within additional sites of disease or in an alternative location within the same site of disease on the basis of intratumoral/intertumoral heterogeneity. Furthermore, repeated treatments may reinforce the previous immunologic anti-tumor immune response through repeated stimulation to previously recognized antigens. We theorize that this could precipitate a robust multidomain abscopal response, complete with affinity maturation, class switching, and somatic hypermutation, given that tumor-specific plasma cells, memory cells, and antigen-presenting cells may be present when the patient has received prior treatments.[39]

Limitations include the retrospective nature of this study, necessitated by multiple factors, including the high cost of medications, the large regulatory burden of using investigational new drugs, and off-label use of established immunotherapy drugs with the intratumoral route of administration. In addition, the heterogeneity of the administered treatment protocols limits the data homogeneity, although this can be attributed in part to rapid advances in drug and technology development. The patient sample is also heterogeneous in nature, with the inclusion of HBV and alcohol-induced cirrhotic patients traveling internationally for treatment. Obtained laboratory studies, and pre/postprocedural imaging protocols were therefore heterogeneous due to availability and local protocols. Finally, imaging equipment and a physician with experience performing image-guided procedures are needed to administer treatment. Future directions include possible clinical trials of pulsed electrical field ablation with intratumoral immunotherapy in the setting of hepatocellular carcinoma. This manuscript may serve as a proof-of-concept to support these efforts. Patient 1 developed transient ascites after treatment, which would be considered as an adverse event, although it is conceivable that hepatic decompensation was a byproduct of an anti-tumor inflammatory cascade. Patient 3 developed transient lactic acidosis and an acute kidney injury posttreatment, both of which ultimately resolved. Given that there were no high-grade toxicities or severe adverse events in our cohort, a clinical trial could potentially recruit advanced patients who are not candidates for other therapies due to medical comorbidities and patients who have failed other lines of therapy. Extensive laboratory testing could be implemented to monitor for biomarkers of systemic immune activation, such as pretreatment and post-treatment cytokine panels, interferon gamma levels, and other investigations. Future trials could potentially include patients with tumor thrombus, given that there was an observed effect against advanced tumor thrombus. In the context of a clinical trial, a standardized treatment protocol would be formulated, and adequate patient follow-up could be assured.

CONCLUSIONS

Pulsed electrical field ablation plus intratumoral immunotherapy may be safe and effective for the treatment of advanced HCC. The liver is an ideal target for locoregional ablation given its percutaneous accessibility. Importantly, intratumoral administration allows for precise administration of lower dosages of immunotherapy medications, which may produce off-target toxicity when administered systemically. Patients may benefit from immunologic tumor elimination, which may be extensive. This treatment does not affect their candidacy for standard of care, including possible liver transplantation, and may downstage or bridge patients to transplantation. If a complete response is obtained, alternatively, a watch-and-wait approach may be appropriate in select patients with regard to surgery. Pulsed electrical field ablation plus intratumoral immunotherapy may be used synergistically with other modalities, including systemic therapy, radiation, and intra-arterial therapies in a combination approach.

CONFLICTS OF INTEREST/FINANCIAL DISCLOSURES

All authors have declared that there are no financial conflicts of interest with regard to this work.

REFERENCES

1. Teufel A, Staib F, Kanzler S, et al. Genetics of hepatocellular carcinoma. *World J Gastroenterol*. 2007;13:2271–2282.
2. El-Serag HB, Rudolph KL. Hepatocellular carcinoma: epidemiology and molecular carcinogenesis. *Gastroenterology*. 2007;132:2557–2576.
3. Gabbia D, De Martin S. Tumor mutational burden for predicting prognosis and therapy outcome of hepatocellular carcinoma. *Int J Mol Sci*. 2023;24:3441.
4. Sha D, Jin Z, Budczies J, et al. Tumor mutational burden as a predictive biomarker in solid tumors. *Cancer Discov*. 2020;10:1808–1825.
5. Pinter M, Pinato DJ, Ramadori P, et al. NASH and hepatocellular carcinoma: immunology and immunotherapy. *Clin Cancer Res*. 2023;29:513–520.
6. Brown ZJ, Tsilimigras DI, Ruff SM, et al. Management of hepatocellular carcinoma: a review. *JAMA Surg*. 2023;158:410–420.
7. Keum H, Albadawi H, Zhang Z, et al. Bioengineered ionic liquid for catheter-directed tissue ablation, drug delivery, and embolization. *Adv Mater*. 2024;36:e2309412.
8. Melssen MM, Fisher CT, Slingluff CL, et al. Peptide emulsions in incomplete Freund's adjuvant create effective nurseries promoting egress of systemic CD4. *J Immunother Cancer*. 2022;10:e004709.
9. Jahrsdörfer B, Weiner GJ. CpG oligodeoxynucleotides as immunotherapy in cancer. *Update Cancer Ther*. 2008;3:27–32.
10. Larson AC, Doty KR, Solheim JC. The double life of a chemotherapy drug: Immunomodulatory functions of gemcitabine in cancer. *Cancer Med*. 2024;13:e7287.
11. Hu J, Li X, Yang L, et al. Hypoxia, a key factor in the immune microenvironment. *Biomed Pharmacother*. 2022;151:113068.

Copyright © 2026 Wolters Kluwer Health, Inc. All rights reserved.

Copyright © 2026 Wolters Kluwer Health, Inc. All rights reserved.

12. Milano G, Innocenti F, Minami H. Liposomal irinotecan (Onivyde): exemplifying the benefits of nanotherapeutic drugs. *Cancer Sci*. 2022;113:2224–2231.
13. Houssein M, Abi Saab W, Khalil M, et al. Cell death by gallotannin is associated with inhibition of the JAK/STAT pathway in human colon cancer cells. *Curr Ther Res Clin Exp*. 2020;92:100589.
14. Razaghi A, Poorebrahim M, Sarhan D, et al. Selenium stimulates the antitumour immunity: Insights to future research. *Eur J Cancer*. 2021;155:256–267.
15. Toomey P, Kodumudi K, Weber A, et al. Intralesional injection of rose bengal induces a systemic tumor-specific immune response in murine models of melanoma and breast cancer. *PLoS One*. 2013;8:e68561.
16. Eberstål S, Badn W, Fritzell S, et al. Inhibition of cyclo-oxygenase-2 enhances immunotherapy against experimental brain tumors. *Cancer Immunol Immunother*. 2012;61:1191–1199.
17. Jiang Z, Sun H, Yu J, et al. Targeting CD47 for cancer immunotherapy. *J Hematol Oncol*. 2021;14:180.
18. Salomon R, Dahan R. Next generation CD40 agonistic antibodies for cancer immunotherapy. *Front Immunol*. 2022; 13:940674.
19. Linch SN, McNamara MJ, Redmond WL. OX40 agonists and combination immunotherapy: putting the pedal to the metal. *Front Oncol*. 2015;5:34.
20. Getu AA, Tigabu A, Zhou M, et al. New frontiers in immune checkpoint B7-H3 (CD276) research and drug development. *Mol Cancer*. 2023;22:43.
21. Graziani G, Tentori L, Navarra P. Ipilimumab: a novel immunostimulatory monoclonal antibody for the treatment of cancer. *Pharmacol Res*. 2012;65:9–22.
22. Kim AMJ, Nemeth MR, Lim SO. 4-1BB: a promising target for cancer immunotherapy. *Front Oncol*. 2022;12:968360.
23. Peng L, Fang Z, Zhang W, et al. Recent advances in colony stimulating factor-1 receptor (CSF1R) inhibitors. *Biochem Pharmacol*. 2025;242(Pt 1):117187.
24. Greene S, Robbins Y, Mydlarz WK, et al. Inhibition of MDSC Trafficking with SX-682, a CXCR1/2 inhibitor, enhances NK-cell immunotherapy in head and neck cancer models. *Clin Cancer Res*. 2020;26:1420–1431.
25. Gu L, Lingeman R, Yakushijin F, et al. The anticancer activity of a first-in-class small-molecule targeting PCNA. *Clin Cancer Res*. 2018;24:6053–6065.
26. Ruffo E, Wu RC, Bruno TC, et al. Lymphocyte-activation gene 3 (LAG3): the next immune checkpoint receptor. *Semin Immunol*. 2019;42:101305.
27. Rajan A, Kim C, Heery CR, et al. Nivolumab, anti-programmed death-1 (PD-1) monoclonal antibody immunotherapy: role in advanced cancers. *Hum Vaccin Immunother*. 2016;12:2219–2231.
28. Fang Z, Jiang J, Zheng X. Interleukin-1 receptor antagonist: an alternative therapy for cancer treatment. *Life Sci*. 2023;335: 122276.
29. Gottschlich A, Endres S, Kobold S. Therapeutic strategies for targeting IL-1 in cancer. *Cancers (Basel)*. 2021;13:477.
30. Soler MF, Abaurrea A, Azcoaga P, et al. New perspectives in cancer immunotherapy: targeting IL-6 cytokine family. *J Immunother Cancer*. 2023;11:e007530.
31. Soule E, Bandyk M, Matteo J. Percutaneous ablative cryoimmunotherapy for micrometastaic abscopal effect: no complications. *Cryobiology*. 2018;82:22–26.
32. Li X, Ramadori P, Pfister D, et al. The immunological and metabolic landscape in primary and metastatic liver cancer. *Nat Rev Cancer*. 2021;21:541–557.
33. Moore WH, Silk M, Bhattacharji P, et al. Early experience with PEF in the setting of recalcitrant stage IV lung cancer. *Lung Cancer*. 2025;204:108575.
34. Arciga BM, Walters DM, Kimchi ET, et al. Pulsed electric field ablation as a candidate to enhance the anti-tumor immune response to immune checkpoint inhibitors. *Cancer Lett*. 2025;609:217361.
35. Dongye Z, Li J, Wu Y. Toll-like receptor 9 agonists and combination therapies: strategies to modulate the tumour immune microenvironment for systemic anti-tumour immunity. *Br J Cancer*. 2022;127:1584–1594.
36. Chiang CL, Chan KSK, Chiu KWH, et al. Complete response to locoregional therapy plus immunotherapy for hepatocellular carcinoma. *JAMA Oncol*. 2024;10:1548–1553.
37. Dawood S, Austin L, Cristofanilli M. Cancer stem cells: implications for cancer therapy. *Oncology (Williston Park)*. 2014;28:1101–1107; 10.
38. Dagogo-Jack I, Shaw AT. Tumour heterogeneity and resistance to cancer therapies. *Nat Rev Clin Oncol*. 2018;15:81–94.
39. Suek N, Campesato LF, Merghoub T, et al. Targeted APC activation in cancer immunotherapy to enhance the abscopal effect. *Front Immunol*. 2019;10:604.

 Copyright © 2026 Wolters Kluwer Health, Inc. All rights reserved.

Copyright © 2026 Wolters Kluwer Health, Inc. All rights reserved.